1521-0103/12/3413-829–839$25.00
THE JOURNAL OF PHARMACOLOGY AND EXPERIMENTAL THERAPEUTICS Vol. 341, No. 3
Copyright © 2012 by The American Society for Pharmacology and Experimental Therapeutics 192245/3772604
JPET 341:829–839, 2012

Heat Shock Protein 25-Enriched Plasma Transfusion Preconditions the Heart against Doxorubicin-Induced Dilated Cardiomyopathy in Mice[S]

Karthikeyan Krishnamurthy, Ragu Kanagasabai, Lawrence J. Druhan, and Govindasamy Ilangovan

Division of Cardiovascular Medicine, Davis Heart & Lung Research Institute, Department of Internal Medicine (K.K., R.K., G.I.), and Department of Anesthesiology (L.J.D.), The Ohio State University, Columbus, Ohio

Received January 30, 2012; accepted March 20, 2012

ABSTRACT

Extracellular heat shock proteins (eHsps) in the circulation have recently been found to activate both apoptotic and protective signaling in the heart. However, the role of eHsps in doxorubicin (Dox)-induced heart failure has not yet been studied. The objective of the present study was to determine how Dox affects circulating eHsp25 in blood plasma and how eHsp25 affects Dox-induced dilated cardiomyopathy. Wild-type mice [HSF-1(+/+)] were pretreated with 100 μl of heterozygous heat shock factor-1 [HSF-1(+/−)] mouse plasma (which contained 4-fold higher eHsp25 compared with wild-type mice), HSF-1(+/+) plasma, or saline, before treatment with Dox (6 mg/kg). After 4 weeks of this treatment protocol, HSF-1(+/−) plasma-pretreated mice showed increased eHsp25 in plasma and improved cardiac function (percentage of fractional shortening 37.3 ± 2.1 versus 26.4 ± 4.0) and better life span (31 ± 2 versus 22 ± 3 days) compared with the HSF-1(+/+) plasma or saline-pretreated mice. Preincubation of isolated adult cardiomyocytes with HSF-1(+/−) plasma or recombinant human Hsp27 (rhHsp27) significantly reduced Dox-induced activation of nuclear factor-κB and cytokine release and delayed cardiomyocyte death. Moreover, when cardiomyocytes were incubated with fluorescence-tagged rhHsp27, a saturation in binding was observed, suggesting that eHsp25 can bind to surface receptors. Competitive assays with a Toll-like receptor 2 (TLR2) antibody reduced the rhHSP27 binding, indicating that Hsp25 interacts with TLR2. In conclusion, transfusion of Hsp25-enriched blood plasma protected the heart from Dox-induced cardiotoxicity. Hsp25 antagonized Dox binding to the TLR2 receptor on cardiomyocytes.

Introduction

The clinical utility of doxorubicin (Dox) is severely limited by the incidence of life-threatening dilated cardiomyopathy among patients who receive a cumulative dose exceeding 550 to 600 mg/m^2 during chemotherapeutic regimens (Minotti et al., 2004; Peng et al., 2005). Even though several pathways such as mammalian target of rapamycin inhibition (Zhu et al., 2009), phosphodiesterase-5 inhibition (Fisher et al., 2005), reduction in circulating progenitor cells (Huang et al., 2010), activation of Toll-like receptors (Nozaki et al., 2004; Riad et al., 2008), impaired metabolism (Maslov et al., 2010), and triggering autophagy (Kobayashi et al., 2010) have been identified, the precise mechanism of Dox-induced cardiotoxicity still remains unclear. We recently identified a novel pathway: that heat shock factor (HSF-1) is activated because of Dox-induced oxidative stress, and this activation enhanced the expression of heat shock proteins including Hsp25 in Dox-treated mouse hearts (Vedam et al., 2010). Systemic stresses, such as genotoxic (i.e., Dox treatment) and proteotoxic (accumulation of denatured proteins) stresses, induce HSF-1 activation and enhance stress-inducible protein expression in eukaryotic cells (Baler et al., 1993; Sarge et al., 1993; Xiao et al., 1999). HSF-1 is activated by diverse forms of stress, and the activation of HSF-1 occurs via a multistep process (Sakamoto et al., 2006). Induction of Hsp25 in Dox-treated hearts was shown to regulate p53 transcriptional activity and expression of the proapoptotic protein Bax

This study was supported in part by the National Institutes of Health National Heart, Lung, and Blood Institute [Grant R21-HL094881].
Article, publication date, and citation information can be found at http://jpet.aspetjournals.org.
http://dx.doi.org/10.1124/jpet.112.192245.
[S] The online version of this article (available at http://jpet.aspetjournals.org) contains supplemental material.

ABBREVIATIONS: Dox, doxorubicin; HSF-1, heat shock factor 1; Hsp, heat shock protein; eHsp, extracellular heat shock protein; TLR, Toll-like receptor; LV, left ventricular; H&E, hematoxylin and eosin; rh, recombinant human; OG-rhHsp27, Oregon Green-labeled recombinant human HSP27; IL-6, interleukin-6; TNF-α, tumor necrosis factor-α; FS, fractional shortening; DAPI, 4,6-diamidino-2-phenylindole; MAPK, mitogen-activated protein kinase; BBI, beat-to-beat interval; NF-κB, nuclear factor-κB.

(Vedam et al., 2010). Many studies have reported that overexpression of small Hsps, such as Hsp27 (the Hsp25 ortholog), protects the heart (Liu et al., 2007; Fan et al., 2008). Paradoxically, however, there is compelling evidence that an elevated level of Hsp25 or Hsp27 is present in failing hearts (Dohke et al., 2006). Thus, it is not clear whether this increase in Hsp27 in the failing human heart (Hsp25 in murine heart) is the result of an unsuccessful protective mechanism or whether the increased expression of Hsp25 indeed potentiates the loss of cardiomyocytes in the heart.

Extracellular Hsps (eHsps), which are present in blood plasma, are being actively studied for their role in innate immunity (Multhoff, 2006; Schmitt et al., 2007; Dhodapkar et al., 2008). Dox has been reported to activate monocytes and macrophages in the circulation and induce an immunogenic response through activation of interleukin-1 family receptors such as Toll-like receptors (TLRs) (Riad et al., 2008). These responses may lead to an increase in eHsps in the circulation, although no systematic study has been performed on the levels of circulating eHsps in Dox-treated experimental animals or in humans. Various receptors, especially the TLRs, present on immune cells such as macrophages and monocytes, have been identified as potential targets for Hsps. Upon binding to these receptors, Hsps were found to activate downstream signaling to enhance cytokine secretion as a part of the immune response. Recent studies have shown that cardiomyocytes express TLRs (Petersen et al., 2005; Boyd et al., 2006), and Hsps can bind to these receptors (Roelofs et al., 2006; Kim et al., 2009). In particular, Hsp60 has been found to competitively bind to TLR4 and enhance apoptosis in cardiomyocytes (Lewthwaite et al., 2002; Kim et al., 2009). TLR2 has been identified as a receptor for Dox, and its deletion was found to be protective against Dox-induced cardiotoxicity (Nozaki et al., 2004). Independent studies have shown that circulating eHsp25 could interact with TLRs and act as a putative ligand (Kardys et al., 2008). Thus, we hypothesized that enhancing circulating eHsp25 would antagonize Dox by competitive binding to TLR and prevent Dox-induced cardiotoxicity. Hence, the objective of this study was to establish the relationship between the plasma level of Hsp25 (eHsp25) and Dox-induced cardiomyopathy and to determine whether circulating eHsp25 could protect the heart from Dox.

Materials and Methods

Animals and Treatment. HSF-1 knockout founders were obtained as a generous gift from Dr. Ivor Benjamin, University of Utah, crossed with BALB/c (Charles River Laboratories, Inc., Wilmington, MA) mice, and genotyped (Vedam et al., 2010). Eight-week-old HSF-1(+/+), HSF-1(+/−), and HSF-1(−/−) mice in the BALB/c background were used in all studies. All the protocols were approved by the institutional animal care and use committee and were performed according to the National Institutes of Health *Guide for the Care and Use of Laboratory Animals* (Institute of Laboratory Animal Resources, 1996). Blood was drawn by cardiac puncture, and plasma was collected with heparin as an anticoagulant. Immunodepletion of Hsp25 in the plasma was carried out by immunoprecipitating Hsp25 from whole plasma, using an anti-Hsp25 antibody. The absence of Hsp25 in the immunodepleted plasma was confirmed by Western blotting before injection into mice. Dox dosing was via bolus intraperitoneal injection of 6 mg/kg b.wt. per week for a total of 4 weeks. This dose was reported to cause Dox-induced heart failure in mice within 4 weeks (Yoshida et al., 2009). Plasma infusion was performed through tail vein cannulation. A detailed description of all of the experimental methods is available in the supplemental data.

Survival and Weight Loss Studies. Two sets of survival studies were performed. In the first set, HSF-1(+/+), HSF-1(+/−), and HSF-1(−/−) mice were injected with Dox, and survival was followed. In the second set, mice were pretreated with saline or HSF-1(+/+) plasma or HSF-1(+/−) plasma followed by Dox. The Kaplan-Meier curve was plotted and analyzed for 50% survival time in each group.

Two-Dimensional Echocardiography. M-mode echocardiography was performed using a GE Vivid 7 ultrasound imaging system (software version 3.4.2; GE Healthcare, GE Healthcare, Chalfont St. Giles, Buckinghamshire, UK) equipped with a 13-MHz linear-array transducer. Two-dimensional short axis echocardiography was performed at the level of the midpapillary muscle. All measurements were averaged from a minimum of three cardiac cycles. LV end-diastolic and end-systolic internal diameters were measured. LV mass and fractional shortening (percentage) were calculated as described before (Vedam et al., 2010).

Immunoblot Analysis. Immunoblotting in whole-cell lysates and immunoprecipitates were performed using routine procedures (Vedam et al., 2010).

Histopathology. To examine histological changes at the end of 4 weeks, hearts were harvested and fixed in 10% neutral buffered formalin, routinely processed, and embedded in paraffin. Paraffin sections were cut into 4-μm serial sections. Counterstaining with hematoxylin and eosin (H&E) was performed.

Immunofluorescence Staining in Heart Tissue by Confocal Microscopy. Tissue sections were incubated with both rabbit anti-α-actin antibody (Abcam, Cambridge, MA) and mouse anti-Hsp25 antibody (Sigma-Aldrich, St. Louis, MO), and the slides were stained with both green Alexa Fluor 488-conjugated goat anti-rabbit secondary antibody and red Alexa Fluor 555-conjugated donkey anti-mouse secondary antibody (Invitrogen, Carlsbad, CA) for fluorescent imaging.

Recombinant Human Hsp27 Expression, Purification, Tagging with Oregon Green Fluorescent Dye and Binding on Cardiomyocytes. Recombinant human (rh) Hsp27 (low-endotoxin, human ortholog of murine Hsp25) was used in the present work because it has been very well established in cardiomyocyte binding studies (Panasenko et al., 2002). Expression and purification of recombinant human Hsp27 were performed as described before (Panasenko et al., 2002). Denaturation and renaturation of Hsp27 were also performed as described before (van de Klundert et al., 1998). rhHsp27 was labeled with Oregon Green 488 according to the manufacturer's protocol (F-6153; Invitrogen). The final labeled protein concentration was quantitated by measuring the absorbance at 280 nm and correcting the absorbance for Oregon Green and the extinction coefficient for Hsp27 (Kim et al., 2009). Cardiomyocytes were incubated with Oregon Green-labeled recombinant human Hsp27 (OG-rhHsp27) with increasing concentrations for 30 min at 4°C and washed, and fluorescence was determined as described by Habich et al. (2002). In competitive assays, the cells were preincubated with anti-TLR2 antibody (Abcam). Dox fluorescence in cardiomyocytes was determined with excitation at 546 nm, measuring emission at 565 nm (Shen et al., 2008).

Cardiomyocyte Beat-to-Beat Interval Studies. Isolated cardiomyocytes were treated with Dox alone or HSF-1(+/−) plasma + Dox, and spontaneous contractions of a single cardiomyocyte (supplemental video) were recorded until the cardiomyocyte in focus lost its rod morphology (becomes rounded). Contractility was manually counted as a function of time from the recorded video, and beat-to-beat interval was determined.

Statistical Analysis. All values are expressed as mean ± S.E. Significance analyses were performed using one-way analysis of variance followed by a post hoc procedure wherever needed, using SPSS software (version 16; SPSS Inc., Chicago, IL). A log-rank test

was applied in Kaplan-Meier curves. Statistical significance was accepted at a value of $P < 0.05$.

Results

Elevation of Circulating Extracellular Hsp25 in Dox-Treated Mice. HSF-1(+/+), HSF-1(+/−), and HSF-1(−/−) mice were treated with Dox (6 mg/kg b.wt.) or the vehicle (saline) for 4 weeks, and circulating plasma eHsp25 was determined. Figure 1A shows the Western blots of eHsp25 in plasma of HSF-1(+/+), HSF-1(+/−), and HSF-1(−/−) mice, after 4 weeks of Dox treatment. Quantitative comparison of the basal eHsp25 level in plasma, determined before the Dox regimen was started (Fig. 1B), showed higher eHsp25 in HSF-1(+/−) (approximately 4-fold) and HSF-1(−/−) (approximately 3-fold) mice, compared with HSF-1(+/+) mice, suggesting that the circulating eHsp25 level is higher in HSF-1(+/−) mice. Given the fact that HSF-1 knockout animals are supposed to show low levels of Hsps including Hsp25, and indeed it was reported so in different tissues of these mice previously (Yan et al., 2002), a higher plasma level of eHsp25 in HSF-1(+/−) mice indicates that some other unknown factors are activating Hsps expression in circulating cells. Previous studies have shown that mutant and wild-type hetero trimers of HSF-1 are transcriptionally more active than the HSF-1 homo trimers (HSF-1 trimers are the active form of the HSF-1 transcriptome) (Voellmy, 2005), which may be responsible for the increased basal level eHsp25 in heterozygous mice.

Upon treatment with Dox, the eHsp25 level progressively increased with each week in HSF-1(+/+) mice (Fig. 1B; Supplemental Fig. 1), whereas in the HSF-1(+/−) and HSF-1(−/−) groups, there was no significant further increase from the already higher basal level (Fig. 1B). The increase in HSF-1(+/+) mice started as early as the 2nd week (Fig. 1B; Supplemental Fig. 1). Of interest, Dox-induced cardiotoxicity, determined in terms of cardiac dysfunction, showed a very minimal change in ejection fraction in the HSF-1(+/−) hearts and only a moderate reduction in HSF-1(−/−) hearts (Supplemental Fig. 2), unlike the severe cardiac dysfunction noted in HSF-1(+/+) mice. Furthermore, the survival analysis of these mice indicated an inverse correlation between survival and basal eHsp25 level (Fig. 1, B and C). The 50% death (log-rank test) was 23 ± 3 days in the HSF-1(+/+) group (lowest basal eHsp25) and 36 ± 4 days in the HSF-1(−/−) group, and, strikingly, no significant death (50% death >100 days) was observed in the HSF-1(+/−) group (highest basal eHsp25).

Because inflammatory cells such as macrophages are known to be activated upon treatment with Dox (Krysko et al., 2011) as an innate immunogenic response, we determined whether there was any increased expression of Hsp25 in macrophages of Dox-treated mice. Intraperitoneal cavity macrophages were isolated from Dox- or saline-treated HSF-1(+/+) and HSF-1(+/−) mice (Fig. 1D) and used for Hsp25 determination. Hsp25, determined by Western blotting, increased (3-fold) in macrophages of Dox-treated HSF-1(+/+) mice (Fig. 1E), compared with saline-treated macrophages. However, in the HSF-1(+/−) group, the macrophages of saline-treated mice showed a very high level of Hsp25 [even higher than that for the Dox-treated HSF-1(+/+) group] (Fig. 1E), and no significant increase was produced by Dox treatment. In macrophages, IL-6 increased upon treatment with Dox in both groups, indicating activation of inflammatory cells (Fig. 1F). We have also found that basal IL-6 was higher in HSF-1(+/−) mice than in HSF-1(+/+) mice (Supplemental Fig. 3). These results suggest that the plasma

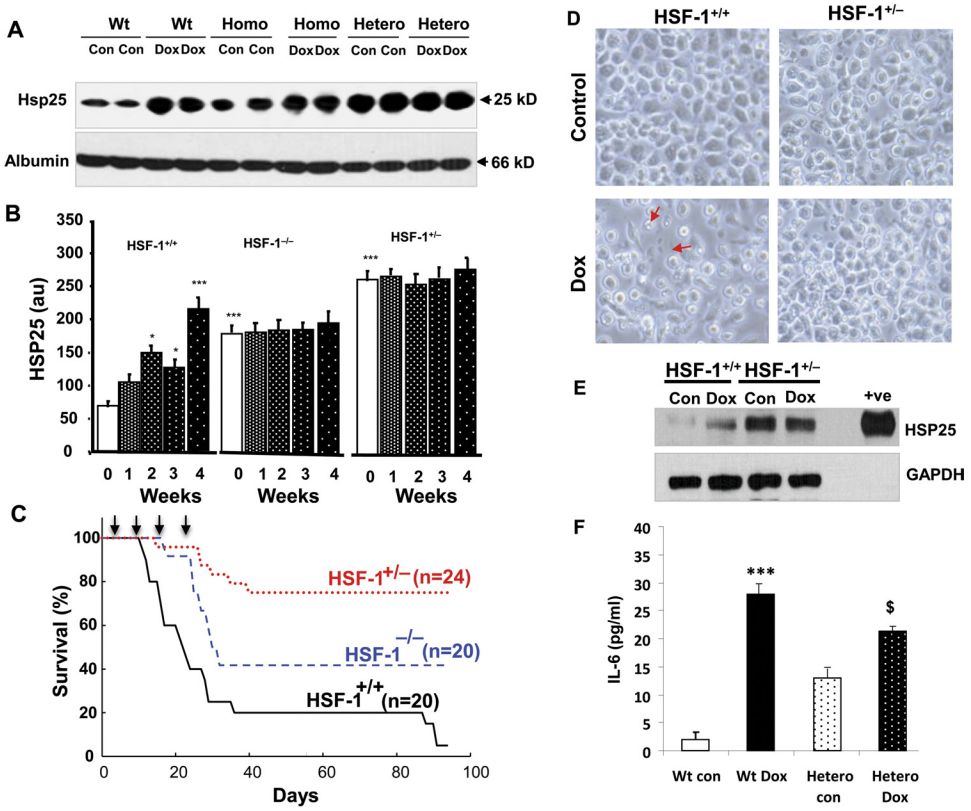

Fig. 1. The plasma level of eHsp25 in Dox-treated mice. A, Western blots of eHsp25 and albumin (loading control), determined in plasma before the start of Dox treatment (i.e., the basal level) and after completion of four doses (over 4 weeks) in HSF-1(+/+), HSF-1(+/−), and HSF-1(−/−) mice. Each group was loaded in duplicate as indicated. B, quantitative analysis of Western blot intensity for various groups (over weeks 1–4) (***, $p < 0.001$; *, $p < 0.01$, compared with the wild-type baseline). A significance test was performed, comparing the control (saline alone-treated) of HSF-1(+/+) mice ($n = 4$ in each group). C, survival curves of Dox-treated HSF-1(+/+), HSF-1(+/−), and HSF-1(−/−) mice as indicated in the figure. D, micrographs of macrophages isolated from Dox- or saline-treated (control) mice. Higher rates of cell death are observed in the macrophages of Dox-treated HSF-1(+/+) mice than in those of HSF-1(+/−) mice [indicated by arrows and independent lactate dehydrogenase measurements (data not included)]. E, representative Western blots of Hsp25 in the macrophages (+ve is the authentic sample control) ($n = 3$). F, IL-6 determination in macrophages (***, $p < 0.001$; $, $p < 0.05$) ($n = 6$). Wt, wild-type; Con, control; Homo, homozygous; Hetero, heterozygous; GAPDH, glyceraldehyde-3-phosphate dehydrogenase.

level of eHsp25 is probably regulated via an immunogenic responsive mechanism, involving monocyte/macrophage cells and that this mechanism is constitutively active in an HSF-1-deficient setting.

HSF-1(+/−) Plasma Transfusion Improves Survival and Attenuates Cytokine Release. Three groups of HSF-1(+/+) wild-type mice were infused with either HSF-1(+/−) plasma (100 μl), HSF-1(+/+) plasma, or an equal volume of saline. Twenty-four hours later, all of these groups were divided into two and infused with either Dox (6 mg/kg) or saline (resulting in six groups: saline alone; saline + Dox; HSF-1(+/+) plasma alone; HSF-1(+/+) plasma + Dox; HSF-1(+/−) plasma alone; and HSF-1(+/−) plasma + Dox). This infusion was repeated for 4 weeks, resulting in four doses of HSF-1(+/−) plasma and Dox (Supplemental Fig. 4). Figure 2A shows survival curves for these six groups. Wild-type mice, treated with HSF-1(+/−) plasma + Dox, showed 50% survival at 31 ± 2 days, which was higher than that for either the HSF-1(+/+) plasma + Dox-treated group (23 ± 4 days) or the saline + Dox-treated group (22 ± 3 days). Moreover, only 60% mortality over 50 days (by the end of the study period) was observed in the HSF-1(+/−) plasma-treated mice, whereas in the HSF-1(+/+) plasma + Dox-treated group or saline + Dox-treated group, more than 80% mortality was observed. Body weight loss induced by Dox as a result of its systemic toxicity was also found to be less for the HSF-1(+/−) plasma-transfused group (Supplemental Fig. 5), illustrating the decreased toxicity in this group. The eHsp25-depleted (by immunoprecipitation using an Hsp25-specific antibody) HSF-1(+/−) plasma transfusion group did not show increased survival, confirming that eHsp25 in plasma is responsible for the enhanced survival of that cohort (Supplemental Fig. 6). Moreover, mice injected with purified rhHsp27 before Dox treatment showed an increase in survival, but the increase was not equal in magnitude to that found for the HSF-1(+/−) plasma treatment group, perhaps because of lipopolysaccharide contamination or denaturing of rhHsp27, causing death among the cohort (Kim et al., 2009). Even though only 100 μl of HSF-1(+/−) plasma was infused four times, a 4-fold increase in eHsp25 was observed (which was not proportional to the infused amount), suggesting that infusion of HSF-1(+/−) plasma enhances the production of eHsp25, potentially through activation of macrophages in the circulation (Fig. 1E). Moreover, the fact that the plasma level of eHsp25 was further elevated (Fig. 2, B and C) in the HSF-1(+/−) plasma + Dox group, despite less systemic toxicity, indicated that HSF-1(+/−) plasma + Dox transfusions primed the secretory mechanism to release more eHsp25 in response to Dox. To test the fact that immune cells are activated upon plasma transfusion, cytokines, namely IL-6 and TNF-α, were determined. Both IL-6 and TNF-α were increased by treatment with HSF-1(+/−) plasma (Fig. 2, D and E). IL-6 showed a 4-fold increase upon treatment with Dox alone, and although there was an increase in IL-6 in the HSF-1(+/−) plasma + Dox-treated groups, the increase was significantly blunted relative to that for the Dox alone-treated group (Fig. 2D). Likewise, HSF-1(+/−) plasma treatment almost completely removed the Dox-induced increase in TNF-α (Fig. 2E).

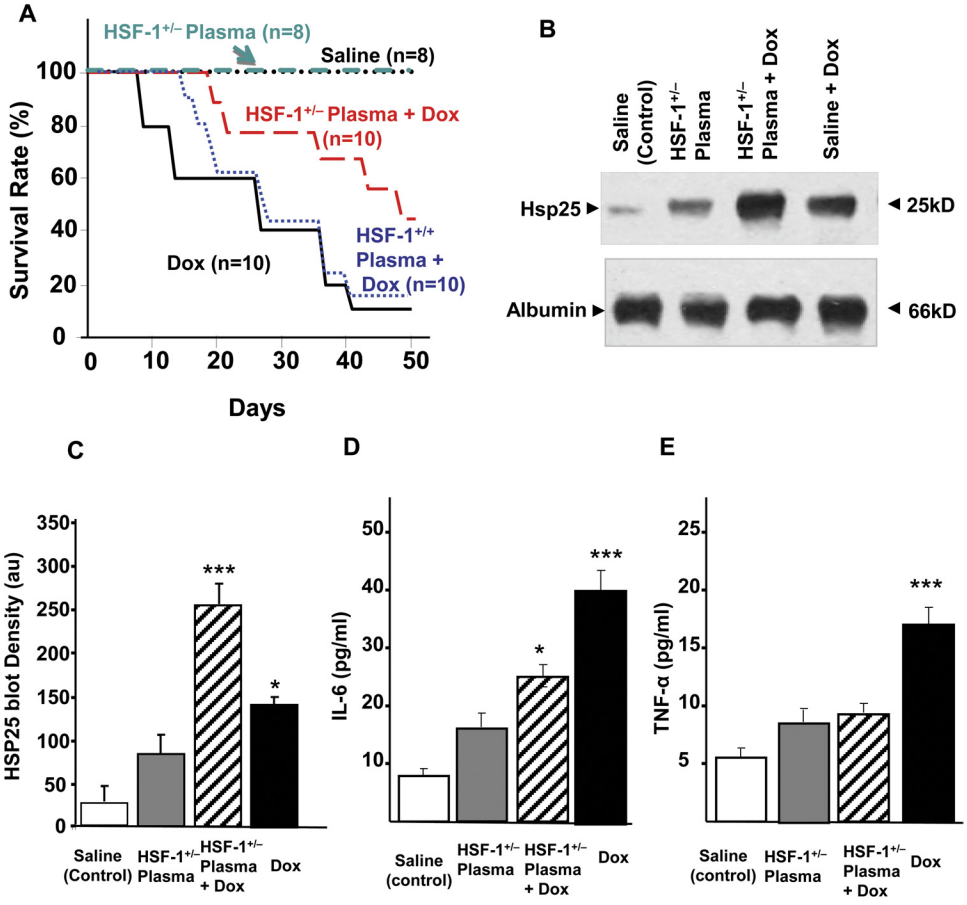

Fig. 2. Effect of HSF-1(+/−) plasma pretreatment and survival against Dox. A, survival curves of saline (100 μl), HSF-1(+/−) plasma (100 μl), HSF-1(+/−) plasma + Dox-treated, saline + Dox (6 mg/kg b.wt.)-treated, and HSF-1(+/+) plasma (100 μl) + Dox-treated groups. B, Western blots of eHsp25 and albumin in plasma as indicated on the image. C, quantitative analysis of Hsp25 blot density in different groups ($n = 3$) (***, $p < 0.001$; *, $p < 0.05$). D and E, IL-6 and TNF-α, measured in plasma of saline-treated, plasma-treated, saline + Dox-treated, and plasma + Dox-treated mice (***, $p < 0.001$; *, $p < 0.05$) ($n = 6$).

Cardioprotection against Dox in HSF-1(+/−) Plasma-Transfused Mice. Figure 3A shows representative echocardiograms of four groups, obtained four weeks after the last dose of Dox. In the HSF-1(+/−) plasma alone- or saline alone-treated groups, cardiac function remained unchanged. The saline + Dox-treated group showed the "dilated cardiomyopathy" phenotype, demonstrated by significant contractile dysfunction observed in the two-dimensional M-mode echocardiograms. The HSF-1(+/+) plasma + Dox-treated group also a showed similar phenotype (data not shown). However, in the HSF-1(+/−) plasma + Dox-treated group, better contractile function relative to that for the other groups was observed (Fig. 3A). The quantitative percentages of fractional shortening (FS), obtained for all the four groups over the study period, are summarized in Fig. 3B. The percentage of FS was 49.4 ± 2 for saline-infused groups. In the saline + Dox-treated group, the percentage of FS decreased to 26.4 ± 4, whereas in the HSF-1(+/−) plasma + Dox-treated group, the percentage of FS was 37.3 ± 2.1, significantly higher than that in the saline + Dox-treated group. Likewise, the LV thickness was significantly higher in the HSF-1(+/−) plasma + Dox group, relative to that in the Dox-treated group (0.66 ± 0.05 and 0.63 ± 0.05 mm, respectively) (Fig. 3C). These results illustrate that the increased survival in the HSF-1(+/−) plasma-pretreated group (Fig. 2A) is probably due to reduced cardiotoxicity. Histopathological evaluation (H&E staining) of LV tissue of all four groups was performed to determine whether there was any reduced tissue damage in the HSF-1(+/−) plasma-pretreated group. The saline or HSF-1(+/−) plasma alone-treated group showed normal myofibrillar structure with striations, branched appearance, and continuity with adjacent myofibrils. The Dox alone-treated group showed extensive myofibrillar degeneration (Fig. 4A). Tissue sections from the HSF-1(+/−) plasma + Dox-treated groups showed normal myofibrillar structure with mild degenerative changes and continuity with adjacent myofibrils (Fig. 4A), and the morphology of cardiac muscle fibers was relatively well preserved. Quantitative assessment of Dox-induced myocardial damage showed a significant decrease in HSF-1(+/−) plasma-pretreated groups (Fig. 4B).

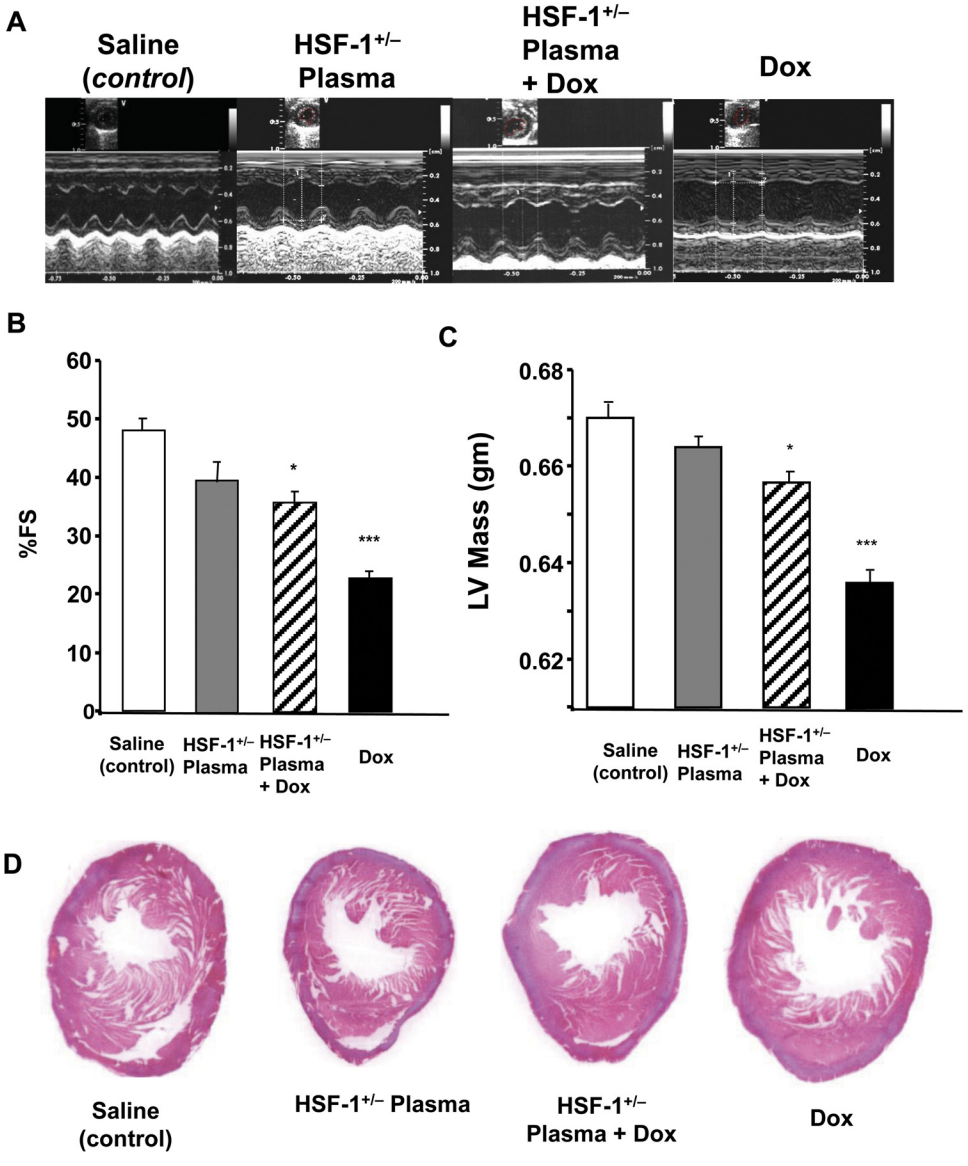

Fig. 3. Echocardiographic evaluation of cardiac dysfunction and histology of Dox-treated mice. A, representative two-dimensional M-mode echocardiogram obtained from saline-treated, HSF-1(+/−) plasma-treated, HSF-1(+/−) plasma + Dox-treated, and saline + Dox-treated mice. B and C, percentage of FS and LV mass determined from echocardiography after 4 weeks of the first dose (***, $p < 0.001$; *, $p < 0.01$) ($n = 6$ in each group). D, representative images of H&E-stained mid-myocardial cross-sections for the four groups ($n = 5$).

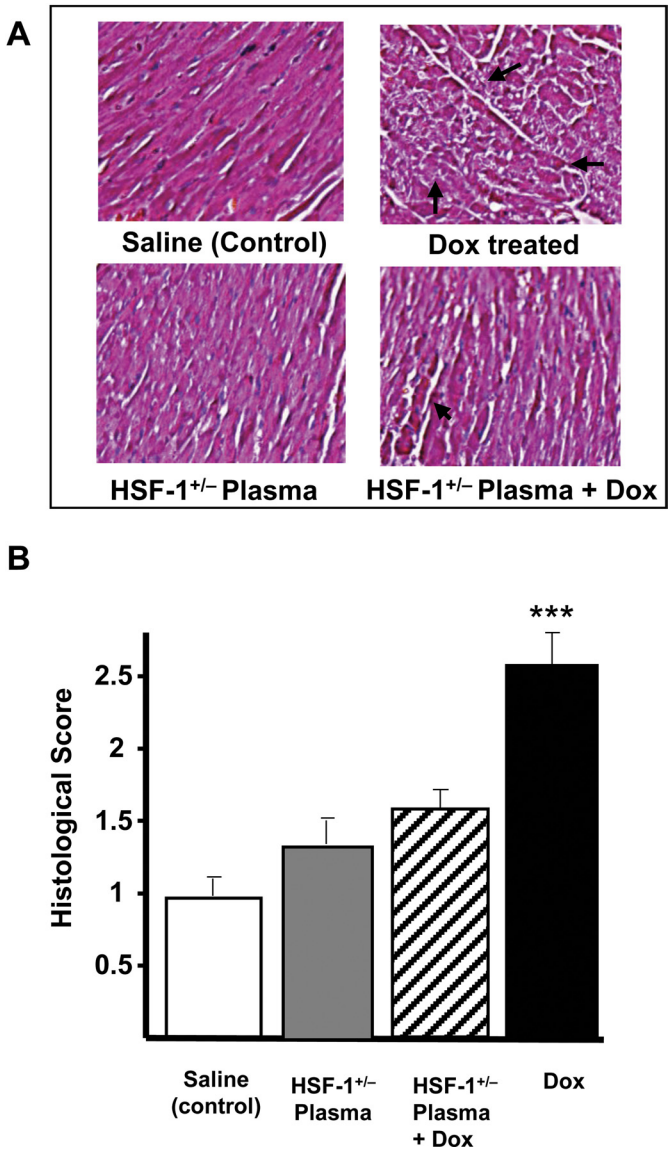

Fig. 4. Plasma attenuated Dox-induced myocardial injury. A, H&E staining of cardiac tissue obtained from saline-treated, HSF-1(+/−) plasma-treated, HSF-1(+/−) plasma + Dox-treated, and saline + Dox-treated mice. B, histological score of Dox-induced myocardial damage in different groups as indicated in the figure (***, $p < 0.001$) ($n = 6$).

HSF-1(+/−) Plasma Transfusion Reduces HSF-1 Activation and Hsp Expression and Suppresses Apoptosis in Dox-Treated Hearts. Western blots and quantitative results for the four major Hsps (Hsp90, Hsp70, Hsp60, and Hsp25, determined in heart tissues after 4 weeks of Dox injection) are presented in Fig. 5. Dox treatment induced all major Hsps and significantly increased them in the heart. Such an enhanced expression of Hsps, as a response to stress has been reported to be due to HSF-1 activation in the heart (Turakhia et al., 2007; Vedam et al., 2010). However, in the HSF-1(+/−) plasma + Dox-treated group, the Hsp levels were very much reduced compared with those in the saline + Dox-treated groups, indicating that HSF-1(+/−) plasma pretreatment inhibited Dox-induced HSF-1 activation in the heart. There was no significant induction of Hsps in the saline alone- or plasma alone-treated groups (Fig. 5, A–C). Although all major Hsps were up-regulated upon treatment with Dox, we focused on Hsp25 because it has been identified as a regulator of p53 activity (Vedam et al., 2010). Immunohistochemical tissue staining was performed in all four groups of hearts to determine whether distribution of Hsp25 expression in the Dox-treated hearts was uniform. Figure 5D summarizes the images of LV tissues stained for Hsp25. As seen, uniform positive staining was confirmed in Dox-treated heart tissues, whereas in the HSF-1(+/−) plasma-pretreated group, Dox treatment did not enhance Hsp25. These results demonstrate that the Dox-induced Hsp expression in the heart is inhibited by HSF-1(+/−) plasma pretreatment, suggesting that the cardioprotection observed in the plasma-pretreated group could be due to inhibition of the HSF-1 activation in these hearts. Further experiments were performed to determine whether these changes in Hsp25 expression occurred in cardiomyocytes. Coregistration of cardio-specific α-actin and Hsp25 was performed. Double immunofluorescence staining and confocal microscopy analysis were used in heart tissues. First, heart tissues were costained with a cardiac muscle α-actin rabbit antibody (Abcam) and an Hsp25 mouse antibody (Sigma-Aldrich), followed by anti-rabbit green fluorescent and anti-mouse Texas red secondary antibodies, and stained with DAPI for nuclei staining. Figure 5E shows microscopic images of fluorescence measured at different excitation and emission, corresponding to the three fluorescent tags and presented as merged images. In Dox-treated mouse hearts, the merged images show largely yellow color (red + green), confirming the overexpression of Hsp25 in cardiomyocytes, whereas Hsp25 was found to be decreased in heart tissues of wild-type mice treated with HSF-1(+/−) plasma alone and with HSF-1(+/−) plasma + Dox (Fig. 5E), as indicated by the greatly decreased yellow intensity. These results confirm that HSF-1(+/−) plasma treatment indeed altered Hsp expression in cardiomyocytes.

Phosphorylated isoforms of myocardial Hsp25, which have been found to play key roles in inducing apoptosis in Dox-treated hearts, were also significantly reduced in the HSF-1(+/−) plasma + Dox-treated group (Fig. 5A). It is known that oxidative stress activates MAPKs in the myocardium, and various MAPKs phosphorylate HSF-1 as well as Hsp25 (Vedam et al., 2010). The p38 MAPK level was, as previously demonstrated, higher in Dox-treated mouse hearts than in saline-treated heart tissue (Fig. 6A). In contrast, the increases in MAPK-activated protein kinase-2 and extracellular signal-regulated kinase 1/2 levels induced in the heart by Dox treatment were significantly attenuated when the mice were treated with HSF-1(+/−) plasma (Fig. 6A). Apoptotic markers were also analyzed in all four groups. First, the p53 level, which has been found to induce Bax in an Hsp25-dependent manner (Stacchiotti et al., 2009), was high in Dox-treated mouse hearts (Fig. 7A), whereas its level was significantly lower in HSF-1(+/−) plasma-pretreated hearts. Likewise, the apoptotic index, defined as the Bax/Bcl2 ratio, was higher in the Dox alone-treated group, relative to the HSF-1(+/−) plasma + Dox-treated group (Fig. 7, A and B). To confirm that attenuation of the Hsp25/p53 apoptotic pathway is indeed responsible for the observed cardioprotection in the HSF-1(+/−) plasma + Dox-treated group, the protein-protein interaction between these proteins was determined. p53 was immunoprecipitated from the lysates of all four

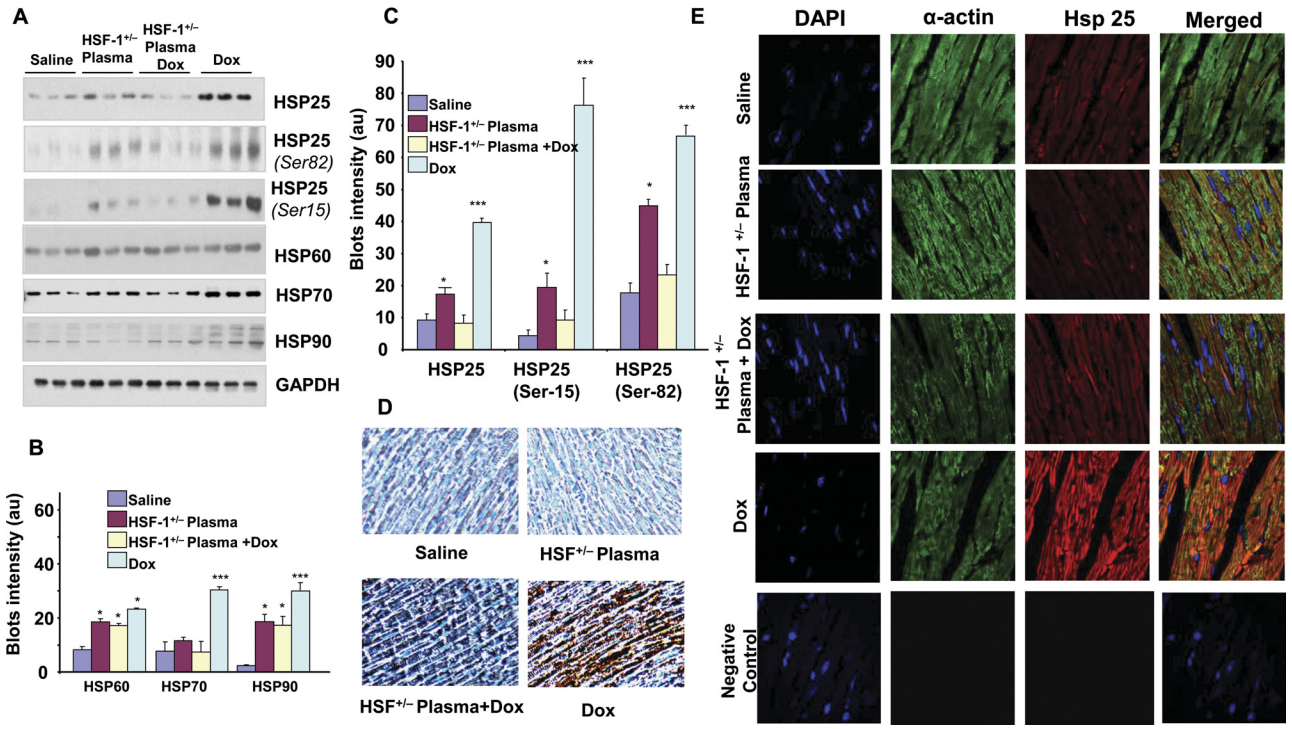

Fig. 5. Attenuation of Dox-induced Hsps in the myocardium by plasma transfusion. A, Western blots of various Hsps, obtained from the myocardial tissue of saline-treated, HSF-1(+/−) plasma-treated, HSF-1(+/−) plasma + Dox-treated, and saline + Dox-treated conditions. B, quantitative analysis of the Western blot intensity of heat shock proteins. (***, $p < 0.001$;*, $p < 0.01$) ($n = 4$). C, quantitative analysis of Hsp25 and its phosphorylated isoforms. D, immunohistochemical staining of Hsp25 in the heart tissue of all the groups ($n = 6$). E, confocal microscopic immunofluorescence coimaging of cardiospecific α-actin and Hsp25 in cardiac tissues. Column 1 is DAPI (blue fluorescence), column 2 is α-actin (green fluorescence), column 3 is Hsp25 (red fluorescence), and column 4 is merged images. Negative control: heart tissues stained with DAPI and Alexa Fluor 488-conjugated goat anti-rabbit secondary antibody and red Alexa Fluor 555-conjugated donkey anti-mouse secondary antibodies ($n = 3$).

groups, and Hsp25 was immunoblotted. Indeed, Hsp25 and S82 phospho Hsp25 showed positive detection; however, relative to the Dox alone-treated group, the blot intensities were very low in the HSF-1(+/−) plasma-pretreated group (Fig. 7C). This finding suggests that Hsp25-dependent apoptotic signaling is very much reduced because of a lack of HSF-1 activation, which is required for p53 transactivation (Vedam et al., 2010).

eHsp25 Antagonizes Dox and Competitively Binds TLR in Cardiomyocytes. The following experiments were performed with isolated adult mouse cardiomyocytes to determine whether the HSF-1(+/−) plasma with higher eHsp25 can protect cardiomyocytes from Dox in vitro. Cardiomyocytes in culture were treated with Dox, and survival was monitored over time. Figure 8A shows the micrographs and Dox fluorescence image of Dox-treated cardiomyocytes. The fluorescence image illustrates that Dox selectively accumulates in nucleus, because of its DNA intercalation property. Viable and healthy isolated mouse adult cardiomyocytes do not typically contract in culture. However, upon addition of Dox, cardiomyocytes start beating, and this can be used as an indicator of Dox toxicity in culture (Schmidt et al., 2007). A delay in the start of beating or prolonged sustained contractility in the presence of Dox and an extended beat-to-beat interval (BBI) is a sign of decreased Dox-induced myocyte death. Cardiomyocyte contraction, after treatment with Dox, was monitored over time until cessation of contractility and transition to the spherical shape common for dead myocytes (supplemental video), and BBI was calculated. Figure 8B shows the quantitative analysis of BBI, as a function of time. Dox alone-treated cardiomyocytes start beating fast and lose rod morphology much faster than myocytes pretreated with HSF-1(+/−) plasma before addition of Dox, clearly illustrating that HSF-1(+/−) plasma protects cardiomyocytes from Dox-induced death.

TLR signaling in Dox-treated myocytes in vitro was assessed from the nuclear fraction of NF-κB. Nuclear translocated NF-κB (p65) was determined by Western blotting and the results obtained are presented in Fig. 8C. Of interest, nuclear translocation of NF-κB was significantly inhibited in HSF-1(+/−) plasma-pretreated cardiomyocytes, suggesting that HSF-1(+/−) plasma pretreatment inhibits the TLR pathway, because TLR activation has been shown to activate the TLR/MyD88/NF-κB pathway. The cytokines IL-6 and TNF-α were also consistently lower in plasma-pretreated myocytes (Fig. 8, D and E). To confirm that eHsp25 binds to the TLR2 receptor on the cell surface, Oregon Green-labeled recombinant human Hsp27 (OG-rhHsp27) was added to isolated cardiomyocytes in culture, and the fluorescence was measured as described previously (Kim et al., 2009). As shown in Fig. 8F, the Oregon Green fluorescence detected showed saturation with an increasing concentration of OG-rhHsp27. Moreover, preincubation with a TLR2 antibody, before addition of OG-rhHsp27, prevented the detected accumulation of Oregon Green fluorescence (Fig. 8F), Together these results indicate that the eHsp25 in HSF-1(+/−) plasma inhibits Dox interaction with the TLR2 receptor and thereby reduces the cardiotoxicity.

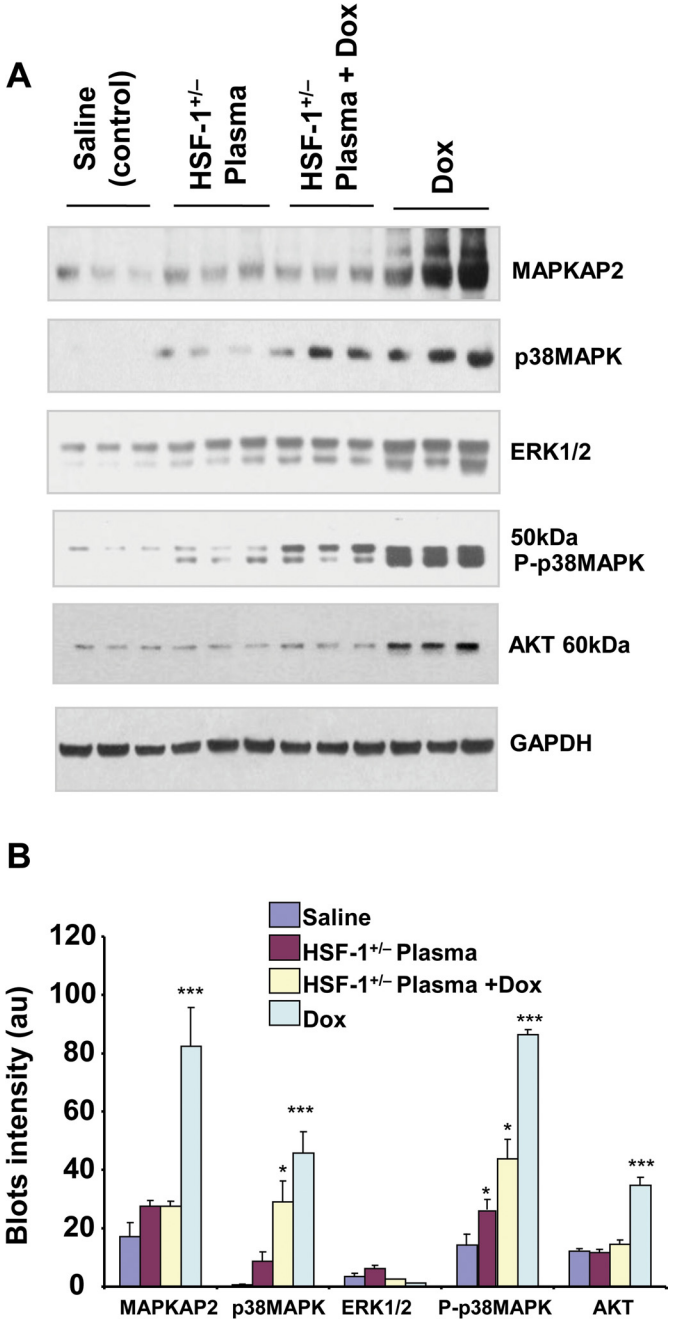

Fig. 6. HSF-1(+/−) plasma pretreatment inhibits Dox-induced MAPKs in the heart. A, Western blots of various MAP kinases for the four groups as indicated on the images. B, quantitative analyses of the blot intensities ($n = 3$) (***, $p < 0.001$; *, $p < 0.01$). ERK1/2, extracellular signal-regulated kinase 1/2; GAPDH, glyceraldehyde-3-phosphate dehydrogenase.

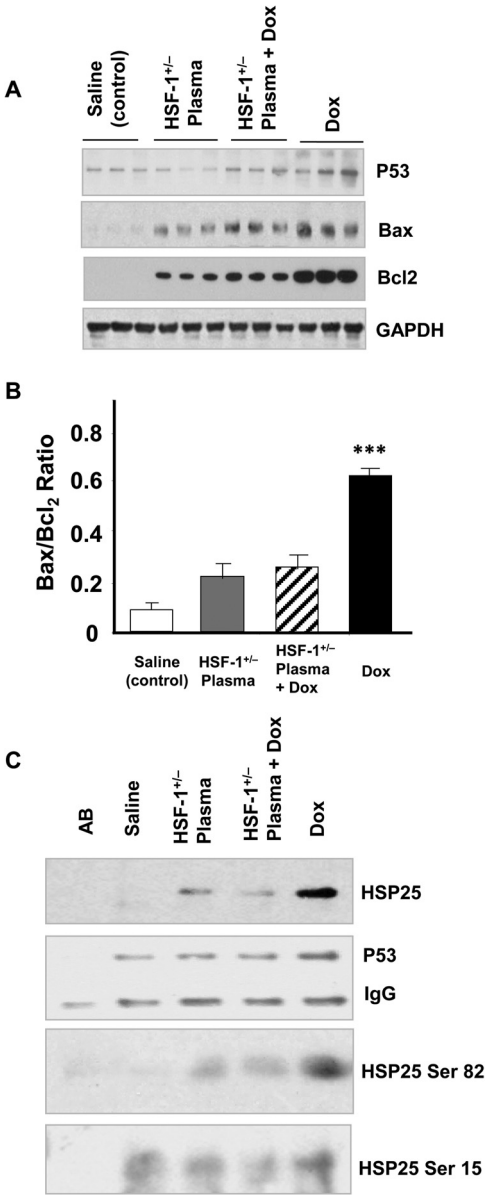

Fig. 7. HSF-1(+/−) plasma pretreatment inhibits Hsp25/p53 interaction in the heart. A, Western blots of various markers as indicated on the images ($n = 3$). B, quantitative analyses of Bax/Bcl2 ratio of the blot intensities. (***, $p < 0.001$). C, Western blots of Hsp25, Ser-82, and Ser-15 phospho Hsp25 in p53 immunoprecipitates from all the four groups. GAPDH, glyceraldehyde-3-phosphate dehydrogenase; AB, control p53 antibody only.

Discussion

Roles for different extracellular Hsps in cardiovascular disease have been the focus of several studies (Kim et al., 2009; Yokota and Fujii, 2010). However, to our knowledge, there are no published data on how Dox affects extracellular heat shock proteins in the circulation and how these circulating eHsps influence Dox-induced heart failure. Our data have demonstrated the novel finding that eHsp25 in the circulation protects against Dox-induced cardiomyopathy by preventing Dox-induced myocyte death. Moreover, our data have shown that preconditioning animals in vivo with plasma containing higher levels of Hsp25, led to an increase in systemic plasma eHsp25, primed the animals for a more robust Dox-induced release of eHsp25 (Fig. 2B), preserved cardiac function after Dox treatment, and increased survival. Hsp25 depletion of the plasma used for pretreatment reversed the observed beneficial effects, and treatment with recombinant Hsp27 largely replicated the increase in survival. Thus, it is clear that when Dox is given in a setting of increased eHsp25, the animal is protected against cardiotoxicity. Of interest, Dox treatment of wild-type animals, which induces cardiac dysfunction and death, also produced an increase in eHsp25, perhaps indicating the activation of some endogenous protective mechanism that failed to protect in some animals.

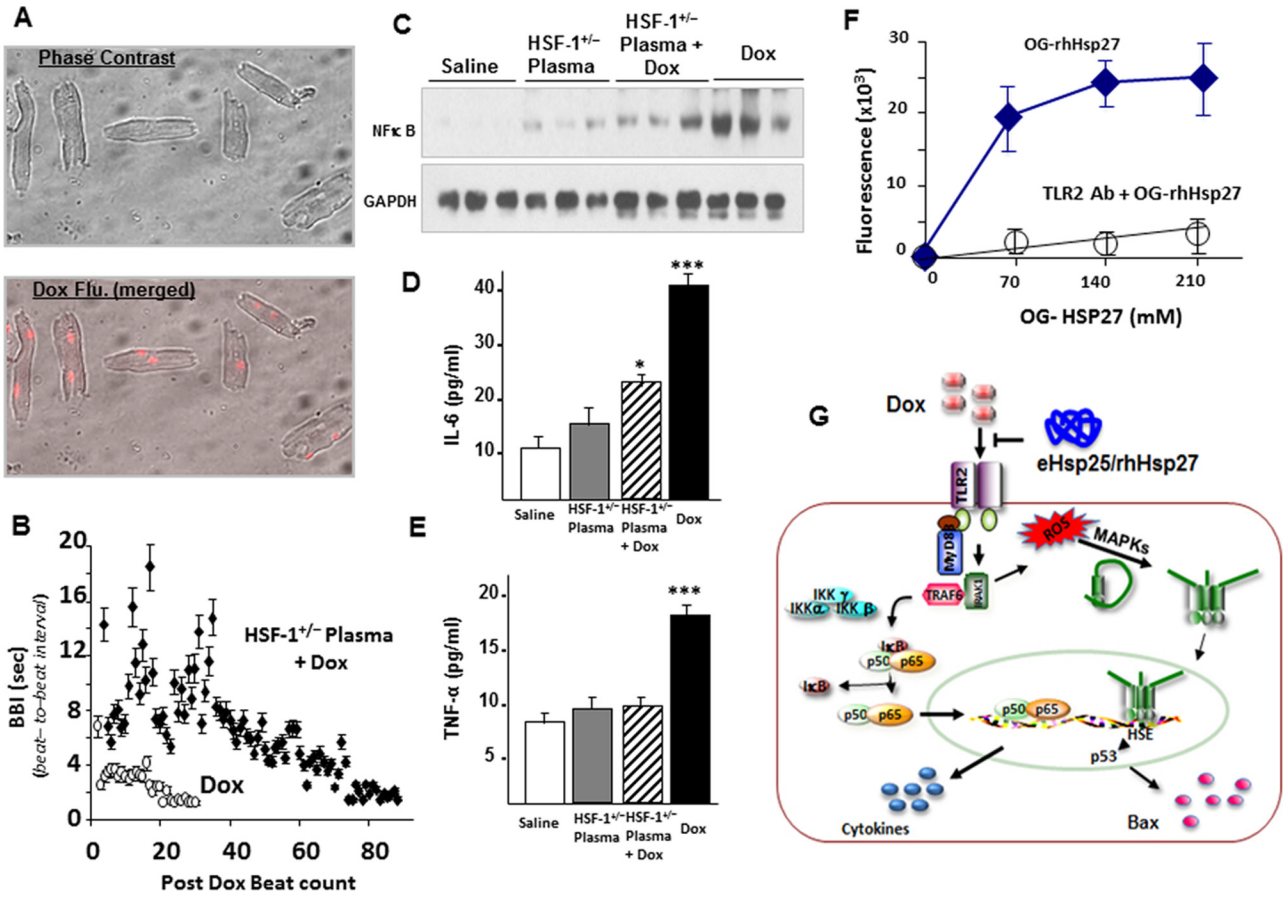

Fig. 8. Dox-induced toxicity and protection by HSF-1(+/−) plasma in adult cardiomyocytes. A, phase-contrast and Dox fluorescence (Flu.) (merged) of Dox-treated myocytes. B, quantitative plots of BBI for cardiomyocytes after addition of Dox in the culture medium ($n = 6$). C, representative Western blots of NF-κB in the nuclear extracts from all the four groups. D and E, IL-6 and TNF-α determined in all the four groups (***, $p < 0.001$; *, $p < 0.01$). F, fluorescence measured in OG-hHsp27 treated and TLR2 antibody (Ab) + OG-hHsp27-treated cardiomyocytes. G, schematic illustration of mechanism of cardioprotection by eHsp25 against Dox in the heart. Dox binding to TLR2 activates the NF-κB-related pathway of apoptosis, as well as MAPKs. This MAPK activation may also be assisted by intracellular redox reaction of Dox to activate HSF-1 and to induce Hsps, particularly Hsp25, which in turn transactivates p53 and expression of Bax (Vedam et al., 2010). If there is a higher level of Hsp25 in the circulation, it can competitively bind to the TLR2 receptors, antagonizing Dox to inhibit Dox-induced apoptotic signaling.

The mechanism by which eHsp25 is produced, either endogenously or in response to Dox, is unclear. In a previous report, Dox was shown to activate stress translation signaling through HSF-1 activation and increased expression of Hsp25 in the myocardium (Vedam et al., 2010). In the present work, we observed that treating HSF-1(+/+) mice with Dox not only increased Hsp25 in the heart but also increased the plasma level of eHsp25 with time, reaching a maximum after 4 weeks when severe cardiac dysfunction was noted. The source of eHsp25 could be excess intracellular Hsps in the cardiomyocytes released into the circulation by some unknown secretory mechanism or macrophage/monocyte release of Hsp25 or a combination of both. In a recent study, Dox was reported to induce an acute immunogenic response by enhancing TLR2 activity in monocytes and macrophages (Krysko et al., 2011). Such a response also showed increased IL-6 in Dox-treated mice. However, it was not determined whether there was a parallel increase in secretion of Hsp25 during this process. We found that both wild-type animals and wild-type cardiomyocytes produce IL-6, TNF-α, and Hsp25 in response to Dox. Thus, it is clear that secretion of Hsp25 accompanies the secretion of immunogenic cytokines. However, when the animals and cardiomyocytes are treated with plasma containing eHsp25, both still demonstrated a Dox-induced increase in IL-6 and TNF-α levels (although blunted in relation to the untreated animals), but only the whole animals showed an increase in Hsp25. These results imply that the source of the eHsp25 is not the cardiomyocyte and that treatment with eHsp25 can regulate the production of Hsp25 in the heart.

How eHsp25/27 could interact with cardiomyocytes or provide cardioprotection in the heart has not been fully elucidated previously, although the plasma level of eHsp27 was studied as a potential marker of atherosclerosis risk in humans (Vivanco et al., 2005; Kardys et al., 2008). Potential correlations between activation of various surface receptors and Dox-induced cardiac injury have been identified (Nozaki et al., 2004). Although activation of receptors such as the hydrocarbon receptor and the androgen receptor reduced Dox-induced cardiotoxicity, activation of other receptors such as CB1 (Mukhopadhyay et al., 2007), ERB1 (Herbst, 2005), and ANG-1A (Leslie et al., 2004) was found to aggravate apoptosis and myocardial remodeling. Genetic knockout and pharmacological inhibition of these receptors have shown cardioprotective effects against Dox-induced heart failure. TLR2 knockout in mice was shown to protect from Dox-induced toxicity, suggesting that activation of TLR2 by Dox could trigger downstream apoptotic signaling in myocytes

(Nozaki et al., 2004). In addition, independent studies have found that Hsp25 interacts with TLR (Kardys et al., 2008). Our results have illustrated for first time that plasma eHsp25 could inhibit the Dox-induced TLR2-related downstream apoptotic signaling and prevent Dox-induced cell death in the heart. Although the present work indicates that eHsp25 is antagonizing Dox by competitive binding to TLR, more work investigating the mechanistic details of other downstream signaling, such as MyD88 activation (Kim et al., 2009), in vivo is warranted. Further studies are ongoing for complete understanding of the overall mechanism.

Taken together, our current findings show that an enhancement of the eHsp25 level in circulation (either by genetic manipulation of HSF-1 or by pharmacologic treatment with Hsp25) can have beneficial consequences for the heart in resisting Dox-induced toxicity via a mechanism involving the antagonism of TLR2. At first glance, these results would seem to oppose our previous findings, that the homozygous HSF-1 knockout, which leads to *decreased* Hsp25 expression in the heart provided cardioprotection via decreased p53 transactivation (Vedam et al., 2010). However, as demonstrated herein, treatment of wild-type mice with eHsp25-containing plasma both increased the eHsp25 level and prevented the induction of Hsp25 expression in the heart. Moreover, the heterozygous HSF-1(+/−) mice, which showed greater survivability when exposed to Dox and were not susceptible to Dox-induced cardiac dysfunction (Supplemental Fig. 2), had a constitutive increase in eHsp25, which was not further increased by the Dox-induced immunogenic activation. Thus, rather than opposing our previous results, our observations can be interpreted in terms of the "heat shock paradox" (DeMeester et al., 2001): that the induction of heat shock proteins can be either beneficial or detrimental, depending on the timing of Hsp induction in relation to injurious insult. If Hsps are increased before injury, either constitutively or pharmacologically induced (as seen in our present work) or by recombinant overexpression (Liu et al., 2007; Fan et al., 2008), there is protection. However, if Hsp25 expression is induced after injury (via HSF-1 activation in response to Dox-induced oxidative stress), it is cytotoxic and aggravates apoptosis in the heart (Vedam et al., 2010). In support of these findings, recent studies by the Knowlton group have demonstrated that TNF-α injury was worsened by HSF-1 activation induced by heat stress after injury (Kobba et al., 2011). Taken together, the accumulated data indicate that overexpression of eHsp25 by any combined therapy during the treatment of cancer using Dox might result in the suppression of cardiomyopathy.

In conclusion, the present work has provided novel insights on the protection of the heart from the effects of Dox by eHsp25-containing plasma. eHsp25 is found to prevent Dox-initiated apoptotic signaling, potentially by antagonizing TLR2. Our recombinant human Hsp27 tagged with Oregon Green showed TLR2 receptor binding, which could be prevented by a TLR2 antibody, clearly showing that eHsp25 antagonized Dox. Furthermore, NF-κB activation (which is caused by TLR2/ligand binding) was decreased in the HSF-1(+/−) plasma-treated hearts (Fig. 8F), suggesting that pretreatment of mice with eHsp25-enriched plasma prevents activation of both the HSF-1 and the NF-κB pathways (Fig. 8G). Heterozygous HSF-1 knockout mice with higher plasma level eHsp25 were highly resistant to Dox-induced heart failure consistently. Therefore, the present study has revealed that a potential therapy based on Hsp25/27 could be developed for clinical applications in the Dox treatment setting and for other applications wherein an antagonist for TLR2 might be beneficial.

Acknowledgments

We gratefully acknowledge Prof. Ivor J. Benjamin, University of Utah, for providing the HSF-1 knockout mice.

Authorship Contributions

Participated in research design: Krishnamurthy, Kanagasabai, Druhan, and Ilangovan.

Conducted experiments: Krishnamurthy and Kanagasabai.

Contributed new reagents or analytic tools: Druhan.

Performed data analysis: Krishnamurthy and Ilangovan.

Wrote or contributed to the writing of the manuscript: Krishnamurthy, Druhan, and Ilangovan.

References

Baler R, Dahl G, and Voellmy R (1993) Activation of human heat shock genes is accompanied by oligomerization, modification, and rapid translocation of heat shock transcription factor HSF1. *Mol Cell Biol* **13:**2486–2496.

Boyd JH, Mathur S, Wang Y, Bateman RM, and Walley KR (2006) Toll-like receptor stimulation in cardiomyocytes decreases contractility and initiates an NF-κB dependent inflammatory response. *Cardiovasc Res* **72:**384–393.

DeMeester SL, Buchman TG, and Cobb JP (2001) The heat shock paradox: does NF-κB determine cell fate? *FASEB J* **15:**270–274.

Dhodapkar MV, Dhodapkar KM, and Li Z (2008) Role of chaperones and FcγR in immunogenic death. *Curr Opin Immunol* **20:**512–517.

Dohke T, Wada A, Isono T, Fujii M, Yamamoto T, Tsutamoto T, and Horie M (2006) Proteomic analysis reveals significant alternations of cardiac small heat shock protein expression in congestive heart failure. *J Card Fail* **12:**77–84.

Fan GC, Zhou X, Wang X, Song G, Qian J, Nicolaou P, Chen G, Ren X, and Kranias EG (2008) Heat shock protein 20 interacting with phosphorylated Akt reduces doxorubicin-triggered oxidative stress and cardiotoxicity. *Circ Res* **103:**1270–1279.

Fisher PW, Salloum F, Das A, Hyder H, and Kukreja RC (2005) Phosphodiesterase-5 inhibition with sildenafil attenuates cardiomyocyte apoptosis and left ventricular dysfunction in a chronic model of doxorubicin cardiotoxicity. *Circulation* **111:**1601–1610.

Habich C, Baumgart K, Kolb H, and Burkart V (2002) The receptor for heat shock protein 60 on macrophages is saturable, specific, and distinct from receptors for other heat shock proteins. *J Immunol* **168:**569–576.

Herbst RS (2005) Role of novel targeted therapies in the clinic. *Br J Cancer* **92 (Suppl 1):**S21–S27.

Huang C, Zhang X, Ramil JM, Rikka S, Kim L, Lee Y, Gude NA, Thistlethwaite PA, Sussman MA, Gottlieb RA, et al. (2010) Juvenile exposure to anthracyclines impairs cardiac progenitor cell function and vascularization resulting in greater susceptibility to stress-induced myocardial injury in adult mice. *Circulation* **121:**675–683.

Institute of Laboratory Animal Resources (1996) *Guide for the Care and Use of Laboratory Animals,* 7th ed, Institute of Laboratory Animal Resources, Commission on Life Sciences, National Research Council, Washington DC.

Kardys I, Rifai N, Meilhac O, Michel JB, Martin-Ventura JL, Buring JE, Libby P, and Ridker PM (2008) Plasma concentration of heat shock protein 27 and risk of cardiovascular disease: a prospective, nested case-control study. *Clin Chem* **54:**139–146.

Kim SC, Stice JP, Chen L, Jung JS, Gupta S, Wang Y, Baumgarten G, Trial J, and Knowlton AA (2009) Extracellular heat shock protein 60, cardiac myocytes, and apoptosis. *Circ Res* **105:**1186–1195.

Kobayashi S, Volden P, Timm D, Mao K, Xu X, and Liang Q (2010) Transcription factor GATA4 inhibits doxorubicin-induced autophagy and cardiomyocyte death. *J Biol Chem* **285:**793–804.

Kobba S, Kim SC, Chen L, Kim E, Tran AL, Knuefermann P, and Knowlton AA (2011) The heat shock paradox and cardiac myocytes: role of heat shock factor. *Shock* **35:**478–484.

Krysko DV, Kaczmarek A, Krysko O, Heyndrickx L, Woznicki J, Bogaert P, Cauwels A, Takahashi N, Magez S, Bachert C, et al. (2011) TLR-2 and TLR-9 are sensors of apoptosis in a mouse model of doxorubicin-induced acute inflammation. *Cell Death Differ* **18:**1316–1325.

Leslie SJ, Johnston N, Strachan FE, Bagnall A, Gray GA, Newby DE, Denvir MA, and Webb DJ (2004) Endothelin-1[1–31] is not elevated in men with chronic heart failure. *J Cardiovasc Pharmacol* **44:**S96–S99.

Lewthwaite J, Owen N, Coates A, Henderson B, and Steptoe A (2002) Circulating human heat shock protein 60 in the plasma of British civil servants: relationship to physiological and psychosocial stress. *Circulation* **106:**196–201.

Liu L, Zhang X, Qian B, Min X, Gao X, Li C, Cheng Y, and Huang J (2007) Over-expression of heat shock protein 27 attenuates doxorubicin-induced cardiac dysfunction in mice. *Eur J Heart Fail* **9:**762–769.

Maslov MY, Chacko VP, Hirsch GA, Akki A, Leppo MK, Steenbergen C, and Weiss RG (2010) Reduced in vivo high-energy phosphates precede Adriamycin-induced cardiac dysfunction. *Am J Physiol Heart Circ Physiol* **299:**H332–H337.

Minotti G, Menna P, Salvatorelli E, Cairo G, and Gianni L (2004) Anthracyclines:

molecular advances and pharmacologic developments in antitumor activity and cardiotoxicity. *Pharmacol Rev* **56:**185–229.
Mukhopadhyay P, Bátkai S, Rajesh M, Czifra N, Harvey-White J, Haskó G, Zsengeller Z, Gerard NP, Liaudet L, Kunos G, et al. (2007) Pharmacological inhibition of CB1 cannabinoid receptor protects against doxorubicin-induced cardiotoxicity. *J Am Coll Cardiol* **50:**528–536.
Multhoff G (2006) Heat shock proteins in immunity. *Handb Exp Pharmacol* **172:** 279–304.
Nozaki N, Shishido T, Takeishi Y, and Kubota I (2004) Modulation of doxorubicin-induced cardiac dysfunction in Toll-like receptor-2-knockout mice. *Circulation* **110:**2869–2874.
Panasenko OO, Seit Nebi A, Bukach OV, Marston SB, and Gusev NB (2002) Structure and properties of avian small heat shock protein with molecular weight 25 kDa. *Biochim Biophys Acta* **1601:**64–74.
Peng X, Chen B, Lim CC, and Sawyer DB (2005) The cardiotoxicology of anthracycline chemotherapeutics: translating molecular mechanism into preventative medicine. *Mol Interv* **5:**163–171.
Petersen CA, Krumholz KA, and Burleigh BA (2005) Toll-like receptor 2 regulates interleukin-1β-dependent cardiomyocyte hypertrophy triggered by *Trypanosoma cruzi*. *Infect Immun* **73:**6974–6980.
Riad A, Bien S, Gratz M, Escher F, Westermann D, Heimesaat MM, Bereswill S, Krieg T, Felix SB, Schultheiss HP, et al. (2008) Toll-like receptor-4 deficiency attenuates doxorubicin-induced cardiomyopathy in mice. *Eur J Heart Fail* **10:**233–243.
Roelofs MF, Boelens WC, Joosten LA, Abdollahi-Roodsaz S, Geurts J, Wunderink LU, Schreurs BW, van den Berg WB, and Radstake TR (2006) Identification of small heat shock protein B8 (HSP22) as a novel TLR4 ligand and potential involvement in the pathogenesis of rheumatoid arthritis. *J Immunol* **176:**7021–7027.
Sakamoto M, Minamino T, Toko H, Kayama Y, Zou Y, Sano M, Takaki E, Aoyagi T, Tojo K, Tajima N, et al. (2006) Upregulation of heat shock transcription factor 1 plays a critical role in adaptive cardiac hypertrophy. *Circ Res* **99:**1411–1418.
Sarge KD, Murphy SP, and Morimoto RI (1993) Activation of heat shock gene transcription by heat shock factor 1 involves oligomerization, acquisition of DNA-binding activity, and nuclear localization and can occur in the absence of stress. *Mol Cell Biol* **13:**1392–1407.
Schmidt H, Saworski J, Werdan K, and Müller-Werdan U (2007) Decreased beating rate variability of spontaneously contracting cardiomyocytes after co-incubation with endotoxin. *J Endotoxin Res* **13:**339–342.
Schmitt E, Gehrmann M, Brunet M, Multhoff G, and Garrido C (2007) Intracellular and extracellular functions of heat shock proteins: repercussions in cancer therapy. *J Leukoc Biol* **81:**15–27.
Shen F, Chu S, Bence AK, Bailey B, Xue X, Erickson PA, Montrose MH, Beck WT, and Erickson LC (2008) Quantitation of doxorubicin uptake, efflux, and modulation of multidrug resistance (MDR) in MDR human cancer cells. *J Pharmacol Exp Ther* **324:**95–102.
Stacchiotti A, Bonomini F, Lavazza A, Rodella LF, and Rezzani R (2009) Adverse effects of cyclosporine A on HSP25, αB-crystallin and myofibrillar cytoskeleton in rat heart. *Toxicology* **262:**192–198.
Turakhia S, Venkatakrishnan CD, Dunsmore K, Wong H, Kuppusamy P, Zweier JL, and Ilangovan G (2007) Doxorubicin-induced cardiotoxicity: direct correlation of cardiac fibroblast and H9c2 cell survival and aconitase activity with heat shock protein 27. *Am J Physiol Heart Circ Physiol* **293:**H3111–H3121.
van de Klundert FA, Smulders RH, Gijsen ML, Lindner RA, Jaenicke R, Carver JA, and de Jong WW (1998) The mammalian small heat-shock protein Hsp20 forms dimers and is a poor chaperone. *Eur J Biochem* **258:**1014–1021.
Vedam K, Nishijima Y, Druhan LJ, Khan M, Moldovan NI, Zweier JL, and Ilangovan G (2010) Role of heat shock factor-1 activation in the doxorubicin-induced heart failure in mice. *Am J Physiol Heart Circ Physiol* **298:**H1832–H1841.
Vivanco F, Martín-Ventura JL, Duran MC, Barderas MG, Blanco-Colio L, Dardé VM, Mas S, Meilhac O, Michel JB, Tuñón J, et al. (2005) Quest for novel cardiovascular biomarkers by proteomic analysis. *J Proteome Res* **4:**1181–1191.
Voellmy R (2005) Dominant-positive and dominant-negative heat shock factors. *Methods* **35:**199–207.
Xiao X, Zuo X, Davis AA, McMillan DR, Curry BB, Richardson JA, and Benjamin IJ (1999) HSF1 is required for extra-embryonic development, postnatal growth and protection during inflammatory responses in mice. *EMBO J* **18:**5943–5952.
Yan LJ, Christians ES, Liu L, Xiao X, Sohal RS, and Benjamin IJ (2002) Mouse heat shock transcription factor 1 deficiency alters cardiac redox homeostasis and increases mitochondrial oxidative damage. *EMBO J* **21:**5164–5172.
Yokota S and Fujii N (2010) Immunomodulatory activity of extracellular heat shock proteins and their autoantibodies. *Microbiol Immunol* **54:**299–307.
Yoshida M, Shiojima I, Ikeda H, and Komuro I (2009) Chronic doxorubicin cardiotoxicity is mediated by oxidative DNA damage-ATM-p53-apoptosis pathway and attenuated by pitavastatin through the inhibition of Rac1 activity. *J Mol Cell Cardiol* **47:**698–705.
Zhu W, Soonpaa MH, Chen H, Shen W, Payne RM, Liechty EA, Caldwell RL, Shou W, and Field LJ (2009) Acute doxorubicin cardiotoxicity is associated with p53-induced inhibition of the mammalian target of rapamycin pathway. *Circulation* **119:**99–106.

Address correspondence to: Dr. Govindasamy Ilangovan, 392 Biomedical Research Tower, The Ohio State University, 460 W. 12th Ave., Columbus, OH 43210. E-mail: govindasamy.ilangovan@osumc.edu